European Journal of
Nuclear
Medicine

Case report

Importance of intra-therapy single-photon emission tomographic imaging in calculating tumour dosimetry for a lymphoma patient

Kenneth F. Koral[1], Kenneth R. Zasadny[1], Fayez M. Swailem[1]*, Steven F. Buchbinder[1], Isaac R. Francis[2], Mark S. Kaminski[1], and Richard L. Wahl[1]

[1] Department of Internal Medicine, Nuclear Medicine Division, and [2] Department of Radiology, University of Michigan, B16412 0028, Ann Arbor, MI 48109, USA

Received 29 October 1990 and in revised form 11 February 1991

Abstract. The dosimetry for two, similarly sized tumours in a lymphoma patient being treated with non-bone marrow ablative, monoclonal antibody therapy is reported. The 45-year-old man was infused with 2.48 GBq (67 mCi) of ^{131}I-labelled MB-1. Prior to therapy, a time series of diagnostic conjugate-view images and a radionuclide transmission scan were obtained and processed to obtain time-activity curves. Starting 2 days after the therapeutic infusion of radioactivity, a second conjugate-view time series was obtained. At that time, a quantitative single-photon emission tomography (SPET) acquisition was also carried out. Pre- and post-therapy X-ray computed tomography scans demonstrated a percentage reduction in volume for the right tumour which was 3.8 times that for the left tumour. In contrast, diagnostic conjugate views by themselves estimated the absorbed dose to be the same for the two tumours. Addition of therapy conjugate-view data increased the right-over-left ratio but only to 1.22. Normalizing either time-activity series by the intra-therapy SPET results increased the ratio to greater than 1.5. We assume here that a differential dose is correct according to the differential tumour shirnkage. One can further assume that the largest ratio corresponds most certainly to the most accurate dosimetric method. Other assumptions are possible. While additional study is essential, data from this patient suggest that the preferred dosimetric method is intra-therapy SPET normalization of either time series.

Key words: Tumour dosimetry – Single-photon emission tomography (SPET) quantification – Lymphoma – Monoclonal antibody – Radionuclide therapy

Eur J Nucl Med (1991) 18:432–435

* Present address: V.A. Medical Center, Tucson, AZ 85723, USA
Offprint requests to: K.F. Koral

Introduction

Therapy of non-Hodgkin's B-cell lymphoma patients with both bone marrow ablative (Press et al. 1989; Eary et al. 1990) and non-bone marrow ablative (Wahl et al. 1990) amounts of ^{131}I-labelled pan B-cell MB-1 monoclonal antibody (Link et al. 1986) is in progress. In both of these trials, the patient is initially imaged with conjugate views over days following a diagnostic administration of activity for estimation of tumour dosimetry (Eary et al. 1989, 1990; Press et al. 1989; Wahl et al. 1990). However, one cannot guarantee that the pharmacokinetics after a therapeutic administration will be the same as after tracer administration. Moreover, two phantom studies indicate that quantification with single-photon emission tomography (SPET) is more accurate than with conjugate views (Bigler 1989; Doherty et al. 1985; Zanzonico et al. 1989).

For a lymphoma patient, we describe here absorbed-dose results for two, similarly sized tumours from the predicted therapy time-activity series based on diagnostic conjugate views. We compare them with those from (1) that time series with the activities normalized by the activities from a single, intra-therapy SPET scan, (2) the time series combined with a late-starting therapy conjugate-view time series and (3) the series in (2) normalized by the SPET scan. Another possibility, use of SPET during diagnostic scanning, was not attempted because of anticipated reconstruction problems with the minimal-count data. Note that our basic quantitative SPET approach has been validated with an anthropomorphic phantom as being accurate within $\pm 13\%$ (Koral et al. 1989). We also measured reduction in volume for the two tumours. We then compared the single reduction-in-volume ratio to the four calculated radiation absorbed-dose ratios.

Case report

The patient studied was a 45-year-old man who was diagnosed with advanced-stage, follicular, mixed large and small cell lymphoma and initially treated by splenectomy and chemotherapy consisting of cyclophosphamide, doxorubicin, vincristine and prednisone. His clinical remission lasted about 2 years, at which time widespread, progressive, bulky lymphadenopathy appeared. A biopsy revealed the tumour to be reactive with MB-1, and the patient was subsequently referred for entry into a Food and Drug Administration (FDA) and IRB approved study of ^{131}I-labelled MB-1 therapy.

Diagnosis. After informed consent, quantitative planar imaging of the patient using a conjugate-view method was performed at 2, 24, 48, 72, 96 and 120 h post-diagnostic infusion of 185 MBq (5 mCi; 40 mg) of ^{131}I-labelled MB-1. Briefly, the method was similar to that of Doherty et al. (1985) and proceeded as follows. Two calibration curves were determined. One gave transmission versus effective thickness and was obtained with a ^{57}Co disc source and a water bath containing various thicknesses of water. The other yielded camera efficiency (geometric mean counts/MBq) as a function of effective thickness. It was determined by imaging a known activity source of ^{131}I centered in various thicknesses of water. A ^{57}Co transmission scan of the patient was taken to determine the effective thickness in the region of the tumour. Tumour regions of interest (ROIs) were drawn on the anterior and posterior emission images as well as background ROIs adjacent to the tumour. The tumour geometric mean count was obtained by subtracting the background and taking the mean. From it and the efficiency corresponding to the effective thickness, the value for each point on the time-activity curves shown in the top panel of Fig. 1 was obtained.

Therapy. Next, 2 days after the therapeutic infusion of 2.48 GBq (67 mCi; 40 mg) of ^{131}I-labelled MB-1, a therapy conjugate-view time series was carried out from 2 to 5 days. At 2 days, a quantitative SPET acquisition was also made with a GE 400 AT gamma-camera plus high-energy collimator, 128 stops and a 21.33-min imaging time.

To enable SPET Compton scatter correction by the dual-energy window method, we employed a 20% photopeak window (nominal setting: 327–400 keV) and a scatter window of the same width (254–326 keV). Before reconstruction, an approximate correction for camera deadtime was also made. For ^{99m}Tc we found that correction by combining the count rates from the two windows and computing a single paralysable model deadtime appears to be acceptable (Zasadny et al. 1990). For ^{131}I in a phantom, monitor-source measurements with the direct window yielded a deadtime of 15.0 μs. For the patient, from the direct-window count rate and this deadtime, the paralysable model estimated the deadtime correction factor to be 1.12. We approximated the desired single deadtime correction factor by this value and multiplied both projection sets by it. After deadtime correction, the scatter projections were subtracted from the photopeak projections using a scatter multiplier ("k" value) of 0.75 (Koral et al. 1990b).

The resultant SPET data were reconstructed by an iterative expecation maximization (EM) algorithm using an independently determined attenuation map and yielding a maximum likelihood (ML) solution (Tsui et al. 1989). Convergence of activity values is obtained after sixteen iterations of this programme. Attenuation maps were extracted from an X-ray computed tomography (CT) scan. The technique involves first reconstructing with no attenuation correction to locate registration landmarks, then superimposing attenuation maps and finally reconstructing again employing attenuation correction based on the maps. The attenuation coefficients at each pixel were extrapolated in energy from 70 keV (the "effective" energy of the CT scan) to 364 keV (Nickoloff et al. 1981). The superimposition was achieved by a shifting and scaling computer programme which utilized the centers (x, y and z) of the two tumours in both modalities as input. One of the resultant images is shown in Fig. 2. A needed SPET camera efficiency measurement for ^{131}I was made using the method detailed previously (Koral et al. 1990a). Absolute tumour activities were then obtained from (1) this efficiency and (2) the counts in ROI determined by a semi-automated, second-derivative, edge-detection programme. The resultant SPET activities in percentage of decay-corrected administered activity for the left and right tumours are shown by two points in the bottom panel of Fig. 1.

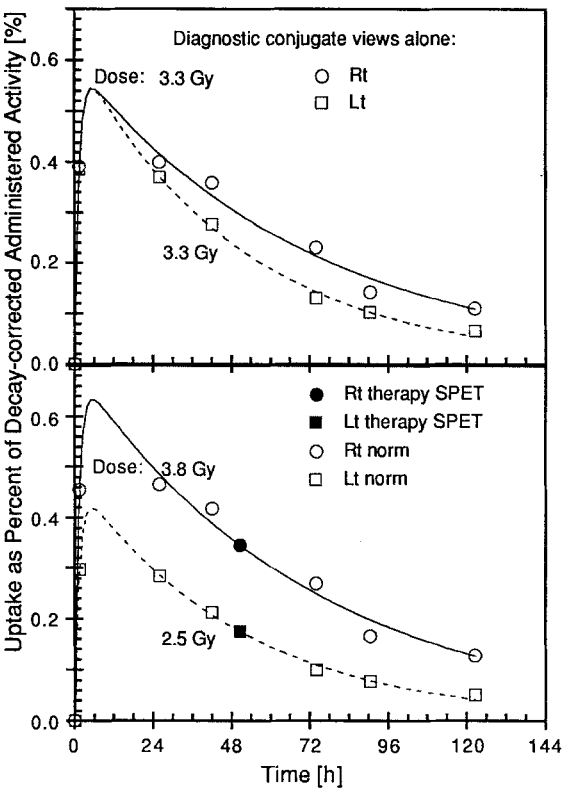

Fig. 1. Time-activity curves for two tumors in a lymphoma patient. At the top are the results from diagnostic conjugate views along with the calculated therapy absorbed dose. At the bottom are the corresponding single-photon emission tomography (SPET) activities measured during therapy and the results after normalizing the diagnostic curves to these values. The new dose is again given. The dose difference between the right and left tumor with normalization agreed better with the post-therapy volume reduction actually observed by CT, assuming that absorbed dose is proportional to the extent of tumor shrinkage

Tumour volumes. Initial tumour volumes for dosimetry were determined from the CT scan taken 8 days before therapy. The patient also had a follow-up CT scan 34 days after therapy, from which post-therapy volumes and reductions in volume were calculated.

Dose calculation. The time-activity data points were fitted by a bi-exponential (see curves in top panel of Fig. 1). From this fit, the dependence of absolute therapy activity on time was calculated.

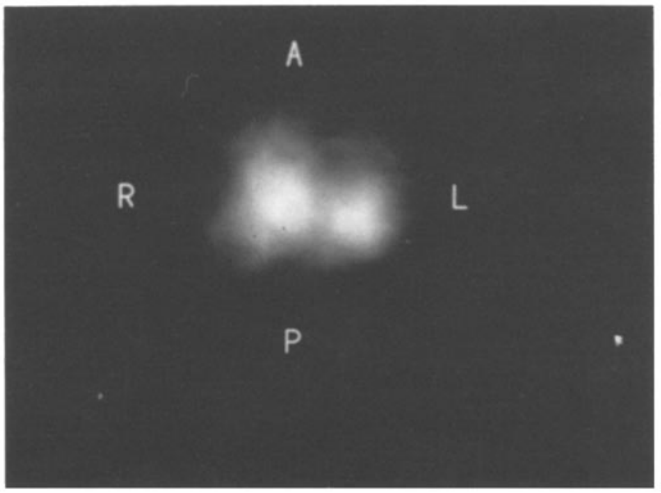

Fig. 2. One transverse slice from the SPET reconstruction of data acquired 48 h after the therapy infusion of ^{131}I-labelled monoclonal antibody. *A*, anterior; *P*, posterior; *L*, left; *R*, right. The "left" tumour is to the patient's left at the right side of the picture

Integrating the function for this dependence from zero to infinity gave the cumulated activity. The SPET-normalized version of a curve was obtained by multiplying each activity by a tumour-specific constant which is chosen so as to allow the normalized curve to pass through the SPET-determined activity. These normalized curves are shown in the bottom panel of Fig. 1. (They, of course, yielded different cumulated activities.)

To use the therapy conjugate-view time series, early points had to be estimated. These were obtained from the early part of the diagnostic series by normalization so that agreement existed at day 2 (the start of the therapy series). Then, bi-exponential fitting yielded a third set of cumulated activities. The final set was calculated by normalizing the combined diagnostic and therapy time series by the SPET results. The radiation absorbed self-dose for each tumour was found from the respective cumulated activity by our implementation of Medical Internal Radiation Dose (MIRD) committee methods (Koral et al. 1989).

Results and discussion

The pre-treatment volume from all pertinent CT slices for the right tumour was 29.6 cm^3 and for the left, 22.6 cm^3. After therapy, the percentage reduction in this volume (the ratio of the difference pre-treatment volume minus post-treatment volume over pre-treatment volume times 100) was 66.9% for the right and 17.6% for the left tumour. That is, the percentage reduction for the right tumour was 3.8 times that for the left.

Absolute values of predicted activities were lower with therapy conjugate views than with diagnostic ones for both tumours. As for curve shape, the time to peak increased about 53% during therapy compared with diagnosis for both tumours. The activity washed out of the right tumour 37% faster during therapy (diagnostic time minus therapy time divided by diagnostic time) but 16% slower for the left (therapy time minus diagnostic time divided by diagnostic time). With therapy conjugate views, our time from peak to half-peak for a 40-mg protein dose can be compared with that for a groin tumour with a 55-mg protein dose (Eary et al. 1990). The average of right, 51.3 h, and left, 36.3 h, is 44 h, exactly equal to the measurement.

Table 1. Calculated radiation absorbed dose as a function of method

Method	Left tumour (Gy)	Right tumour (Gy)	Right-over-left ratio
Diagnostic conjugate views	3.30	3.29	1.00
Intra-therapy SPET-normalized diagnostic conjugate views	2.54	3.83	1.51
Combined diagnostic and therapy conjugate views	1.69	2.07	1.22
Intra-therapy SPET-normalized combined diagnostic and therapy conjugate views	2.46	3.80	1.54

The effect of the SPET deadtime correction was to increase the calculated activities by 15%. Importantly, as seen in Fig. 1, SPET normalization tended to separate the time-activity curves pertaining to the left and right tumours.

The resultant radiation-absorbed dose values for all four procedures are shown in Table 1. It is seen that the right-over-left absorbed-dose ratio is 1.00 with diagnostic conjugate views alone. It increases to 1.22 with the combination of diagnostic and therapy conjugate views possibly due to differences in pharmacokinetics. With intra-therapy SPET normalization of either of the two, the ratio jumps to greater than 1.5 possibly reflecting increased accuracy with SPET. We assume a dose ratio greater than 1.0 is correct because the tumour shrinkage ratio is greater than 1.0. The proportionality constant of the assumed relationship between shrinkage ratio and dose ratio is not known, however. In addition, there are errors in the four calculated dose ratios which we assume are somewhat comparable. We then tentatively conclude that the largest dose ratio corresponds most probably to the most accurate dosimetric method: intra-therapy SPET normalization of either conjugate-view time series.

Above, we have assumed that tumour volume reduction serves as a good index of radiation dose. However, tumour volume regression may not reflect clonogenic cell kill, which is presumably coupled to dose. Interphase cell killing (of clonogenic and non-clonogenic cells) has been adduced as a possible mechanism to explain the

apparent cell loss at relatively low radiation dose in lymphoma; the non-clonogenic cell kill may differentially affect tumours of the same size, leading to variable cell loss and hence volume reduction for the same clonogenic cell kill. A superior radiation dose index might be the time taken for tumour regrowth (Kallman 1987), but it is not available for this patient.

Acknowledgements. This work was supported by PHS grant number RO1 CA38790 and PO CA42768 awarded by the National Cancer Institute, Department of Health and Human Services (DHHS). We appreciate the imaging help from Jon Johnson and Scott Moon, the advice about causes of tumour volume reduction given by one of the reviewers, the reference on the same subject from Dr. Ted Lawrence, M.D., Department of Radiation Oncology, as well as the secretarial assistance of Mrs. Patricia Haines.

References

Bigler RE (1989) "Final Report" for 3 year NIH National Cancer Institute radiation research program contract (contract no. N01-CM37565). Dose calculations for cancer therapy using radioactively labeled antibodies to a tumor-associated and/or tumor-specific antigens. Cornell University Medical College, New York, pp 63–150

Doherty P, Schwinger R, King M, Gionet M (1985) Distribution and dosimetry of indium-111 labeled $F(ab')_2$ fragments in humans. Fourth international radiopharmaceutical dosimetry symposium, Nov 5–8, 1985, Oak Ridge, TN, CONF-851113-(DE86010102)

Eary JF, Appelbaum FL, Durack L, Brown P (1989) Preliminary validation of opposing view method for quantitative gamma camera imaging. Med Phys 16(3):382–387

Eary JF, Press OW, Badger CC, Durack LD, Richter KY, Addison SJ, Krohn KA, Fisher DR, Porter BA, Williams DL, Martin PJ, Appelbaum FR, Levy R, Brown SL, Miller RA, Nelp WB, Bernstein ID (1990) Imaging and treatment of B-cell lymphoma. J Nucl Med 31:1257–1268

Kallman RF (ed) (1987) Rodent tumor models. Pergamon, New York

Koral KF, Wang X, Sisson JC, Botti J, Meyer L, Mallette S, Glazer GM, Adler RS (1989) Calculating radiation absorbed dose for pheochromocytoma tumors in 131-I MIBG therapy. Int J Radiat Oncol Biol Phys 17:211–218

Koral KF, Swailem FM, Buchbinder S, Clinthorne NH, Rogers WL, Tsui BMW (1990a) SPET dual-energy-window Compton correction: scatter multiplier required for quantification. J Nucl Med 31:90–98

Koral KF, Swailem FM, Clinthorne NH, Rogers WL, Tsui BMW (1990b) Dual-window Compton-scatter correction in phantoms: errors and multiplier dependence on energy. J Nucl Med 31:798–799 (abstr)

Link M, Bindl J, Meeker TC, Carswell C, Doss CA, Warnke RA, Levy R (1986) A unique antigen on mature B cells defined by a monoclonal antibody. J Immunol 137:3013–3018

Nickoloff EL, Perman WH, Esser PD, Bashist B, Alderson PO (1981) Left ventricular volume: physical basis for attenuation corrections in radionuclide determinations. Radiology 152:511–515

Press OW, Eary JF, Badger CC, Martin PJ, Appelbaum FR, Levy R, Miller R, Brown S, Nelp WB, Krohn KA, Fisher D, DeSantes K, Porter B, Kidd P, Thomas ED, Bernstein ID (1989) Treatment of refractory non-Hodgkin's lymphoma with radiolabeled MB-1 (anti-CD37) antibody. J Clin Oncol 7(8):1027–1038

Tsui BMW, Gullberg GT, Edgerton ER, Ballard JG, Perry JR, McCartney WH, Berg J (1989) Correction of nonuniform attenuation in cardiac SPET imaging. J Nucl Med 30:497–507

Wahl R, Fig L, Zasadny K, Koral K, Francis I, Miller R, Buchsbaum D, Kaminski M (1990) Radioimmunotherapy of B-cell lymphoma with I131 MB-1 monoclonal antibody. J Nucl Med 31:852 (abstr)

Zanzonico P, Bigler R, Sgouros G, Strauss A, Becker D (1989) Quantitative SPET in radiation dosimetry. Semin Nucl Med XIX:47–61

Zasadny KR, Koral KF, Swailem FM, Rogers WL (1990) Deadtime of an anger camera in dual-energy-window-acquisition mode. J Nucl Med 31:759–760 (abstr)